

3D SURFACE MATCHING WITH MUTUAL INFORMATION AND RIEMANN SURFACE STRUCTURES

Yalin Wang
Mathematics Department
UCLA
email: ylwang@math.ucla.edu

Ming-Chang Chiang
Laboratory of Neuro Imaging
Department of Neurology
UCLA School of Medicine
email: mcchiang@ucla.edu

Paul M. Thompson
Laboratory of Neuro Imaging
Department of Neurology
UCLA School of Medicine
email: thompson@loni.ucla.edu

ABSTRACT

Many medical imaging applications require the computation of dense correspondence vector fields that match one surface with another. Surface-based registration is useful for tracking brain change, registering functional imaging data from multiple subjects, and for creating statistical shape models of anatomy. To avoid the need for a large set of manually-defined landmarks to constrain these surface correspondences, we developed an algorithm to automate the matching of surface features. It extends the mutual information method to automatically match general 3D surfaces (including surfaces with a branching topology). We use diffeomorphic flows to optimally align the Riemann surface structures of two surfaces. First, we use holomorphic 1-forms to induce consistent conformal grids on both surfaces. High genus surfaces are mapped to a set of rectangles in the Euclidean plane, and closed genus-zero surfaces are mapped to the sphere. Next, we compute stable geometric features (mean curvature and the conformal factor) and pull them back as scalar fields onto the 2D parameter domains. Mutual information is used as a cost functional to drive a fluid flow in the parameter domain that optimally aligns these surface features. A diffeomorphic surface-to-surface mapping is then recovered that matches anatomy in 3D. Lastly, we present a spectral method that ensures that the grids induced on the target surface remain conformal when pulled through the correspondence field. Using the chain rule, we express the gradient of the mutual information between surfaces in the conformal basis of the source surface. This finite-dimensional linear space generates all conformal reparameterizations of the surface. Illustrative experiments show the method applied to hippocampal surface registration, a key step in subcortical shape analysis in Alzheimer's disease and schizophrenia.

KEY WORDS

Surface Matching, Riemann Surface Structure, Mutual Information, Brain Mapping

1 Introduction

Surface models are widely used in medical imaging to assist in data visualization, nonlinear image registration, and surface-based signal processing or statistics. Surface models are often generated in computational anatomy studies

to support computations, e.g. when statistically combining or comparing 3D anatomical models across subjects, or mapping functional imaging parameters onto anatomical surfaces. Often the comparison of data on two anatomical surfaces is required, and a correspondence field must be computed to register one surface nonlinearly onto the other. Multiple surfaces can be registered nonlinearly to construct a mean shape for a group of subjects, and deformation mappings can encode shape variations around the mean. This type of deformable surface registration has been used to detect developmental and disease effects on brain structures such as the corpus callosum and basal ganglia [1], the hippocampus [2], and the cortex [3]. Nonlinear matching of brain surfaces can also be used to track the progression of neurodegenerative disorders such as Alzheimer's disease [2], to measure brain growth in development [1], and to reveal directional biases in gyral pattern variability [4].

Surface registration has numerous applications, but a direct mapping between two 3D surfaces is challenging to compute. Often, higher order correspondences must be enforced between specific anatomical points, curved landmarks, or subregions lying within the two surfaces. One common way to achieve this is to first map each of the 3D surfaces to canonical parameter spaces such as a sphere [5, 6] or a planar domain [7]. The surface correspondence problem can then be addressed by computing a flow in the parameter space of the two surfaces [1, 8], which induces a correspondence field in 3D. This flow can be constrained using anatomic information in the form of landmark points or curves, or by constraining the mapping of surface regions represented implicitly using level sets [7]. Feature correspondence between two surfaces can be optimized by using the L^2 -norm to measure differences in convexity [5]. Artificial neural networks can rule out or favor certain types of feature matches [9]. Finally, correspondences may be determined by using a minimum description length (MDL) principle, based on the compactness of the covariance of the resulting shape model [10]. Anatomically homologous points can then be forced to match across a dataset. Thodberg [11] identified problems with early MDL approaches and extended them to an MDL appearance model, as a means to perform unsupervised image segmentation.

By the Riemann uniformization theorem, all surfaces

can be conformally embedded in a sphere, a plane or a hyperbolic space. The resulting embeddings form special groups. Using holomorphic 1-forms and critical graphs, global conformal parameterization [12] can also be used to conformally map any high genus surface (i.e., a surface with branching topology) to a set of rectangular domains in the Euclidean plane. In this paper, we show how to use conformal parameterizations to assist in the matching of arbitrary 3D anatomical surfaces. Mutual information is used to drive a diffeomorphic fluid flow that is adjusted to find appropriate surface correspondences in the parameter domain. Differential geometric features are aligned in this study we chose the mean curvature and the conformal factor of the surfaces, as these are intrinsic and stable. These choices are purely illustrative. In fact, any scalar fields defined on the surfaces could be matched, e.g. cortical thickness maps, or even functional imaging signals or metabolic data. Since conformal mapping and fluid registration techniques generate diffeomorphic mappings, the 3D shape correspondence established by composing these mappings is also diffeomorphic (i.e., provides smooth one-to-one correspondences).

We also present a spectral approach for ensuring that the grid induced on the target surface by the correspondence field, remains conformal. Grid orthogonality is advantageous for accurate numerical discretization of PDEs or for signal processing on the resulting surface meshes. For high genus surfaces, the global conformal parameterization is not unique and all the conformal parameterizations form a linear space. The degrees of freedom in this space of conformal grids are tuned to maximize the mutual information energy of features between the two surfaces. Because the conformal structure is intrinsic and the conformal parameterization continuously depends on the Riemannian metric on the surface, our method is also stable and computationally efficient.

1.1 Previous Work

Several variational or PDE-based methods have been proposed for matching surfaces. Surfaces may be represented by parametric meshes [5], level sets, or both representations [7]. Gu et al. [13] found a unique conformal mapping between any two genus zero manifolds by minimizing the harmonic energy of the map. Gu and Vemuri [14] also matched 3D shapes by first conformally mapping them to a canonical domain and aligning their 2D representations over the class of diffeomorphisms. They demonstrated their algorithm on genus zero closed surfaces.

The mutual information (MI) method [15] measures the statistical dependence of the voxel intensities between two images. This measure of agreement can be used to tune the parameters of a registration transform such that MI is maximal when the two images are optimally aligned. The MI method has been successful for rigid [16] and non-rigid [17, 18] image registration. Here, we generalize it to match 3D surfaces. For MI to work, a mono-

tonic mapping in grayscales between images is not required, so images from different modalities can be registered [19]. Hermosillo et al. [20] adopted linear elasticity theory to regularize the variational maximization of MI. D’Agostino et al. [21] extended this approach to a viscous fluid scheme allowing large local deformations, while maintaining smooth, one-to-one topology [22].

2 Theoretical Background

2.1 Global Conformal Parameterization

Suppose M_1, M_2 are two surfaces. Locally they can be represented as $r_1(x^1, x^2), r_2(x^1, x^2)$, where (x^1, x^2) are their local coordinates, and $r_1, r_2 : R^2 \rightarrow R^3$ are vector-valued functions. The first fundamental form of M_1 is $ds_1^2 = \sum_{ij} g_{ij} dx^i dx^j$, where $g_{ij} = \frac{\partial r_1}{\partial x^i} \cdot \frac{\partial r_1}{\partial x^j}$, $i, j = 1, 2$. Similarly, the first fundamental form of M_2 is defined in the same way: $ds_2^2 = \sum_{ij} \tilde{g}_{ij} dx^i dx^j$. Define a mapping $f : M_1 \rightarrow M_2$ between two surfaces. Using local coordinates, f can be represented as $f : R^2 \rightarrow R^2$, $f = (f^1(x^1, x^2), f^2(x^1, x^2))$. Then any tangent vector (dx^1, dx^2) on M_1 will be mapped to a tangent vector df on M_2 ,

$$\begin{pmatrix} df^1 \\ df^2 \end{pmatrix} = \begin{pmatrix} \frac{\partial f^1}{\partial x^1} & \frac{\partial f^1}{\partial x^2} \\ \frac{\partial f^2}{\partial x^1} & \frac{\partial f^2}{\partial x^2} \end{pmatrix} \begin{pmatrix} dx^1 \\ dx^2 \end{pmatrix} \quad (1)$$

The length of df is $\sum_{m,n} \tilde{g}_{mn} df^m df^n$. We use the length of df to define the length of (dx^1, dx^2) . Namely, we define a new metric for M_1 which is induced by the mapping f and the metric on M_2 . We call this metric *the pull-back metric*, and denote it by $f^* ds_2^2$. Replacing df^m in the above equation by (1), we get the analytic formula for the pull-back metric,

$$f^* ds_2^2 = \sum_{mn} \left(\sum_{ij} \tilde{g}_{ij} (f(x^1, x^2)) \frac{\partial f^m}{\partial x^i} \frac{\partial f^n}{\partial x^j} \right) dx^m dx^n. \quad (2)$$

We call f a *conformal mapping*, if there exists a positive scalar function $\lambda(x^1, x^2)$, such that $f^* ds_2^2 = \lambda(x^1, x^2) ds_1^2$, where $\lambda(x^1, x^2)$ is called the *conformal factor*.

Intuitively, all the angles on M_1 are preserved on M_2 . Figure 1 shows a conformal mapping example. Figure 1(a) shows a hippocampal surface. We conformally map it to a square as in 1(c) and get its conformal parameterization. We illustrate the conformal parameterization via the texture mapping of a checkerboard in Figure 1.

An *atlas* is a collection of consistent coordinate charts on a manifold, where transition functions between overlapping coordinate charts are smooth.

We treat R^2 as isomorphic to the complex plane, where the point (u, v) is equivalent to $z = u + iv$, and $(u, -v)$ is equivalent to $\bar{z} = u - iv$. Let S be a surface in \mathbb{R}^3 with an atlas $\{(U_\alpha, z_\alpha)\}$, where (U_α, z_α) is a chart, and $z_\alpha : U_\alpha \rightarrow \mathbb{C}$ maps an open set $U_\alpha \subset S$ to the complex plane \mathbb{C} .

An atlas is called *conformal* if (1). each chart (U_α, z_α) is a conformal chart. Namely, on each chart, the first fundamental form can be formulated as $ds^2 =$

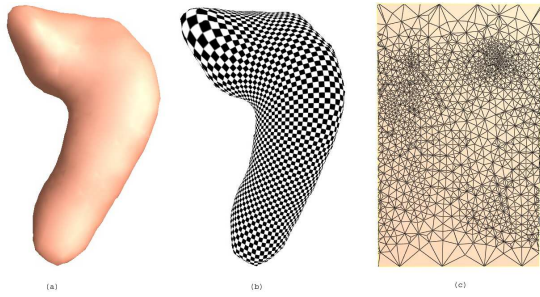


Figure 1. Illustrates conformal surface parameterization. (a) shows a hippocampal surface. (b) shows a conformal parameterization of the hippocampal surface. (c) shows the surface triangulation conformally mapped to a rectangle in the plane. Right angles in the checkerboard are well preserved on the surface in (b).

$\lambda(z_\alpha)^2 dz_\alpha d\bar{z}_\alpha$; **(2)**, the transition maps $z_\beta \circ z_\alpha^{-1} : z_\alpha(U_\alpha \cap U_\beta) \rightarrow z_\beta(U_\alpha \cap U_\beta)$ are holomorphic.

A chart is compatible with a given conformal atlas if adding it to the atlas again yields a conformal atlas. A *conformal structure (Riemann surface structure)* is obtained by adding all compatible charts to a conformal atlas. A *Riemann surface* is a surface with a conformal structure.

One coordinate chart in the conformal structure introduces a *conformal parameterization* between a surface patch and the image plane. The conformal parameterization is angle-preserving and intrinsic to the geometry, and is independent of the resolution and triangulation.

Locally, a surface patch is covered by a conformal coordinate chart. For high genus surfaces, the local conformal parameterization can be extended to cover the whole surface except at several points. These exceptional points are called *zero points*. By the Riemann-Roch theorem, there are $2g - 2$ zero points on a global conformal structure of a genus g closed surface. By the circle-valued Morse theorem, the iso-parametric curves through the zero points segment the whole surface to patches, where each patch is either a topological disk, or a cylinder. The segmentation is determined by the conformal structure of the surface and the choice of the global conformal parameterization.

Figure 2 shows an example of the conformal parameterization of a lateral ventricle surface of a 65-year-old HIV/AIDS patient. We introduce 5 cuts on the surface and change the ventricular surface to a genus 4 surface. The 5 cuts are the blue lines in (a). The conformal structure of the ventricular surface is shown in (b). (c) shows a partition of the ventricular surface, where each segment is labeled by a unique color. (d) shows the parameterization domain. Each rectangle is the image, in the parameterization domain, of a surface component in (c).

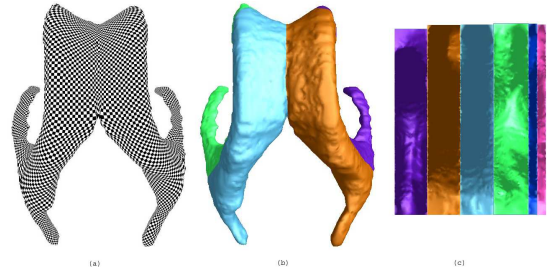


Figure 2. Illustrates conformal parameterization for a high genus surface. (a) shows the conformal structure of a lateral ventricular surface. (b) shows a partition of this surface, with a unique color labeling each part. (c) shows the parameterization domain. Each surface component in (b) is conformally mapped to a rectangle in (c). The color scheme shows the association between elements in (b) and (c).

2.2 Optimal Global Conformal Parameterization

Given a Riemann surface S with a conformal atlas $\{(U_\alpha, z_\alpha)\}$, a holomorphic 1-form ω is defined by a family $\{(U_\alpha, z_\alpha, \omega_\alpha)\}$, such that **(1)**, $\omega_\alpha = f_\alpha(z_\alpha) dz_\alpha$, where f_α is holomorphic on U_α , and **(2)**, if $z_\alpha = \phi_{\alpha\beta}(z_\beta)$ is the coordinate transformation on $U_\alpha \cap U_\beta (\neq \emptyset)$, then $f_\alpha(z_\alpha) \frac{dz_\alpha}{dz_\beta} = f_\beta(z_\beta)$, i.e., the local representation of the differential form ω satisfies the chain rule.

For a Riemann surface S with genus $g > 0$, all holomorphic 1-forms on S form a complex g -dimensional vector space ($2g$ real dimensions), denoted by $\Omega^1(S)$. The conformal structure of a higher genus surface can always be represented in terms of a holomorphic one-form basis, which is a set of $2g$ functions $\omega_i : K_1 \rightarrow \mathbb{R}^2, i = 1, 2, \dots, 2g$. Any holomorphic one-form ω is a linear combination of these functions. The quality of a global conformal parameterization for a high genus surface is fundamentally determined by the choice of the holomorphic 1-form.

Figure 3 shows two different conformal parameterizations of a lateral ventricle surface of a 21-year-old control subject. (a) shows a uniform parameterization result and (b) shows a nonuniform parameterization result. Note that although both of these are conformal, one has greater area distortion than the other.

2.3 Conformal Representation of a General Surface

For a general surface S , we can compute conformal coordinates (u, v) to parameterize S . Based on these coordinates, one can derive scalar fields including the conformal factor, $\lambda(u, v)$, and mean curvature, $H(u, v)$, of the surface position vector $S(u, v)$:

$$\frac{\partial S}{\partial u} \times \frac{\partial S}{\partial v} = \lambda(u, v)n(u, v) \quad (3)$$

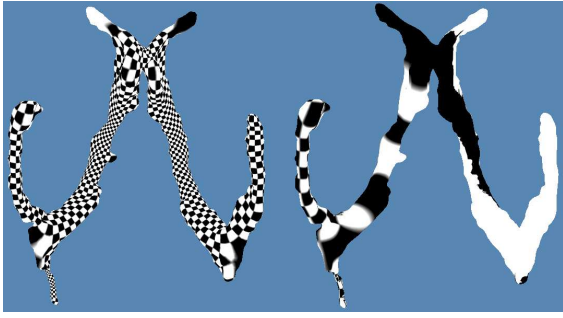


Figure 3. Illustrates optimal global conformal parameterization. On the left, a uniform global conformal parameterization is shown. A non-uniform global conformal parameterization, for the same surface, is shown on the right.

$$H(u, v) = \left| \frac{1}{\lambda^2(u, v)} \left(\frac{\partial^2}{\partial u^2} + \frac{\partial^2}{\partial v^2} \right) r(u, v) \right| \quad (4)$$

We can regard the tuple (λ, H) as the conformal representation of $S(u, v)$. We have the following theorem [23].

Theorem 2.1 *A closed surface $S(u, v)$ in R^3 with conformal parameter (u, v) is uniquely determined by its conformal factor $\lambda(u, v)$ and its mean curvature $H(u, v)$ up to rigid motions. A simply connected surface $r(u, v)$ with a boundary in R^3 and conformal parameter (u, v) is determined by its conformal factor $\lambda(u, v)$ and its mean curvature $H(u, v)$ and the boundary position.*

Clearly, various fields of scalars or tuples could be used to represent surfaces in the parameter domain. Because the conformal structure is intrinsic and independent of the data resolution and triangulation, we use the conformal representation, $\lambda(u, v)$ and $H(u, v)$, represent the 3D surfaces. This representation is stable and computationally efficient.

2.4 Mutual Information for Surface Registration

We now describe the mutual information functional used to drive the scalar fields $\lambda(u, v)$ and $H(u, v)$ into correspondence, effectively using the equivalent of a 2D image registration in the surface parameter space (i.e., in conformal coordinates). Let I_1 and I_2 be the target and the deforming template images respectively, and $I_1, I_2 : R^2 \rightarrow R$. Let $\Omega \subset R^2$ be the common parameter domain of both surfaces (if both are rectangular domains, the target parameter domain can first be matched to the source parameter domain using a 2D diagonal matrix). Also, let u be a deformation vector field on Ω . The MI of the scalar fields (treated as 2D images) between the two surfaces is defined by

$$I(u) = \int_{R^2} p_u(i_1, i_2) \log \frac{p_u(i_1, i_2)}{p(i_1)p_u(i_2)} di_1 di_2 \quad (5)$$

where $p(i_1) = P(I_1(x) = i_1)$, $p_u(i_2) = P(I_2(x - u) = i_2)$ and $p_u(i_1, i_2) = P(I_1(x) = i_1 \text{ and } I_2(x - u) = i_2)$.

We adopted the framework of D’Agostino et al. [21] to maximize MI with viscous fluid regularization. Briefly, the deforming template image was treated as embedded in a compressible viscous fluid governed by the Navier-Stokes equation for conservation of momentum [22], simplified to a linear PDE:

$$Lv = \mu \nabla^2 v + (\lambda + \mu) \vec{\nabla}(\vec{\nabla} \cdot v) + F(x, u) = 0 \quad (6)$$

Here v is the deformation velocity, and μ and λ are the viscosity constants. Following the derivations in [21], we take the first variation of $I(u)$ with respect to u , and use the Parzen window method [24] to estimate the joint probability density function (pdf) $p_u(i_1, i_2)$. The driving force $F(x, u)$ that registers features in the 2D surface parameter space is given by

$$F(x, u) = \frac{1}{A} [L_u(i_1, i_2) * \frac{\partial \Psi_h}{\partial i_2}] (I_u(x), I_2(x - u)) \nabla I_2(x - u) \quad (7)$$

where A is the area of the parameter domain Ω , $L_u(i_1, i_2) = 1 + \log \frac{p_u(i_1, i_2)}{p(i_1)p_u(i_2)}$, $\Psi_h(i_1, i_2) = \phi_h(i_1)\phi_h(i_2) = (\sqrt{2\pi}h)^{-1} \cdot \exp(-i_1^2/2h^2) \cdot (\sqrt{2\pi}h)^{-1} \cdot \exp(-i_2^2/2h^2)$ as the Parzen kernel, and “*” denotes convolution.

3 The Surface Mutual Information Method for an Arbitrary Genus Surface

Next, suppose we want to match two high genus surfaces (i.e., surfaces with the same branching topology). To apply our surface mutual information method piecewise, we first compute the conformal representations of the two surfaces based on a global conformal parameterization. Mutual information driven flows are then applied to align the computed conformal representations, while enforcing constraints to guarantee continuity of the vector-valued flow at the patch boundaries. When the chain rule is used, we can further optimize the mutual information matching results by optimizing the underlying global conformal parameterization.

Let S_1 and S_2 be two surfaces we want to match and the conformal parameterization of S_1 is τ_1 , conformal parameterization for S_2 is τ_2 , $\tau_1(S_1)$ and $\tau_2(S_2)$ are rectangles in R^2 . Instead of finding the mapping ϕ from S_1 to S_2 directly, we can use mutual information method to find a diffeomorphism $\tau : D_1 \rightarrow D_2$, such that the diagram below commutes: $\tau_2^{-1} \circ \tau \circ \tau_1 = \phi$. Then the map ϕ can be obtained by the following commutative diagram,

$$\begin{array}{ccc} S_1 & \xrightarrow{\phi} & S_2 \\ \tau_1 \downarrow & & \downarrow \tau_2 \\ R^2 & \xrightarrow{\tau} & R^2 \end{array} \quad (8)$$

$\phi = \tau_1 \circ \tau \circ \tau_2^{-1}$. Because τ_1 , τ and τ_2 are all diffeomorphisms, ϕ is also a diffeomorphism.

4 Experimental Results

To make the results easier to illustrate, we chose to encode the profile of surface features using a compound scalar function $C(u, v) = 8\lambda(u, v) + H(u, v)$. We linearly normalized its dynamic range to the pixel intensity range 0 to 255. Several examples are shown, mapping one hippocampal surface to another. This type of deformable surface registration is important for tracking developmental and degenerative changes in the hippocampus, as well as computing average shape models with appropriate boundary correspondences. Figure 4 (a) shows the matching fields for several pairs of surfaces, establishing correspondences between distinctive features.

Here geometric features on 3D hippocampal surface, conformal factor and mean curvature, were conformally flattened to a 2D square. In the 2D parameter domain, data from a healthy control subject was registered to data from several Alzheimer’s disease patients. Each mapping can be used to obtain a reparameterization of the 3D surface of the control subject, by convecting the original 3D coordinates along with the flow. Importantly, in Figure 4 (a), some consistent 3D geometric features are identifiable in the 2D parameter domain; bright areas (arrows) correspond to high curvature features in the hippocampal head.

Although validation on a larger sample is required, we illustrate the approach on left hippocampal surface data from one healthy control subject and five patients with Alzheimer’s disease. We register the control subject’s surface to each patient, generating a set of deformation mappings. Figure 4 (b)-(e) show the correspondences as a 3D vector field map connecting corresponding points on two surfaces being registered. (d) and (e) are a part of surface before and after the registration. After reparameterization, a leftward shift in the vertical isocurves adds a larger tangential component to the vector field. Even so, the deformed grid structure remains close to conformal. The lengths of the difference vectors are reduced after the MI based alignment; a formal validation study in a larger sample is now underway.

5 Conclusion and Future Work

We extended the mutual information method to match general surfaces. This has many applications in medical imaging. Our examples of matching various hippocampal surfaces are relevant for mapping how degenerative diseases affect the brain, as well as building statistical shape models to detect the anatomical effects of disease, aging, or development. The hippocampus is used as a specific example, but the method is general and is applicable in principle to other brain surfaces such as the cortex.

Surface-based mutual information automates the matching of surfaces by computing a correspondence field guided by the joint distribution of features lying in both surfaces. This is a natural idea, in that it uses conformal parameterization to transform a surface matching problem

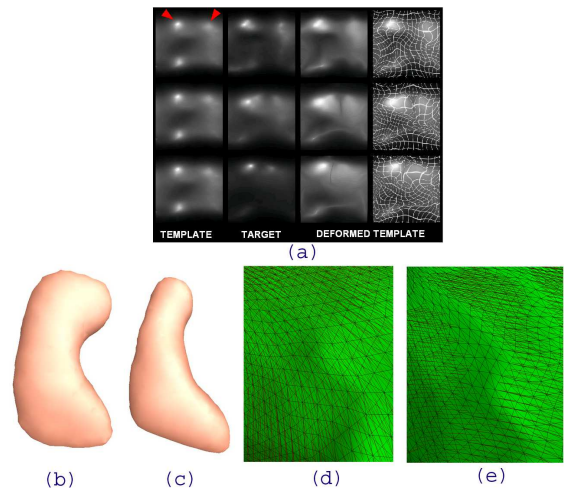


Figure 4. (a) Geometric features on 3D hippocampal surfaces (the conformal factor and mean curvature) were computed and compound scalar fields were conformally flattened to a 2D square. In the 2D parameter domain, data from a healthy control subject (the template, leftmost column) was registered to data from several Alzheimer’s disease patients (target images, second column). The deformed template images are shown in the third and fourth (gridded) columns. (b)-(c) show the two 3D hippocampal surfaces being matched, for (b) a control subject and (c) an Alzheimer’s disease patient. We flow the surface from (b) to (c). (d)-(e) show the 3D vector displacement map, connecting corresponding points on the two surfaces, (d) before and (e) after reparameterization of the source surface using a fluid flow in the parameter domain. These 3D vector fields store information on geometrical feature correspondences between the surfaces.

into an image registration problem. Whether or not this approach provides more relevant correspondences than those afforded by other criteria (minimum description length, neural nets, or hand landmarking) requires careful validation for each application. Optimal correspondence depends more on utility for a particular application than on anatomical homology. Because different correspondence principles produce different shape models, we plan to compare them in future for detecting group differences in brain structure. If statistical power is increased in group comparisons, this would support the use of correspondence fields established by mutual information on surfaces.

References

- [1] P.M. Thompson, J.N. Giedd, R.P. Woods, D. MacDonald, A.C. Evans, and A.W. Toga. Growth patterns in the developing brain detected by using continuum-mechanical tensor maps. *Nature*, 404(6774):190–193, March 2000.

- [2] J.G. Csernansky, S. Joshi, L.E. Wang, J. Haller, M. Gado, J.P. Miller, U. Grenander, and M.I. Miller. Hippocampal morphometry in schizophrenia via high dimensional brain mapping. *Proc. Natl. Acad. Sci.*, 95:11406–11411, September 1998.
- [3] P.M. Thompson, R.P. Woods, M.S. Mega, and A.W. Toga. Mathematical/computational challenges in creating population-based brain atlases. In *Human Brain Mapping*, volume 9, pages 81–92, Feb. 2000.
- [4] G.L. Kindlmann, D.M. Weinstein, A.D. Lee, A.W. Toga, and P.M. Thompson. Visualization of anatomic covariance tensor fields. In *Proc. IEEE Engineering in Medicine and Biology Society (EMBS)*, San Francisco, CA, Sept. 1-5 2004.
- [5] B. Fischl, M.I. Sereno, R.B.H. Tootell, and A.M. Dale. High-resolution inter-subject averaging and a coordinate system for the cortical surface. In *Human Brain Mapping*, volume 8, pages 272–284, 1999.
- [6] M. Bakircioglu, S. Joshi, and M.I. Miller. Landmark matching on brain surfaces via large deformation diffeomorphisms on the sphere. In *Proc. SPIE Medical Imaging*, 1999.
- [7] A. Leow, C.L. Yu, S.J. Lee, S.C. Huang, R. Nicolson, K.M. Hayashi, H. Protas, A.W. Toga, and P.M. Thompson. Brain structural mapping using a novel hybrid implicit/explicit framework based on the level-set method. *NeuroImage*, Feb. 2005.
- [8] C. Davatzikos. Spatial normalization of 3d brain images using deformable models. *Comp. Assisted Tomography*, 20(4):656–665, 1996.
- [9] A. Pitiot, H. Delingette, and P.M. Thompson. Learning object correspondences with the observed transport shape measure. In Ambleside Taylor C, Noble A, editor, *Proc. IPMI 2003*, 2003.
- [10] R.H. Davis, C.J. Twining, T.F. Cootes, J.C. Waterton, and C.J. Taylor. A minimum description length approach to statistical shape modeling. In *IEEE Trans Med. Imaging*, volume 21, pages 525–537, 2002.
- [11] Hans Henrik Thodberg. Minimum description length shape and appearance models. In *IPMI*, pages 51–62, 2003.
- [12] X. Gu and S.T. Yau. Computing conformal structures of surfaces. *Communication of Information and Systems*, December 2002.
- [13] X. Gu, Y. Wang, T.F. Chan, P.M. Thompson, and S.-T. Yau. Genus zero surface conformal mapping and its application to brain surface mapping. *IEEE Trans. on Med. Imaging*, 23(8):949–958, Aug. 2004.
- [14] X. Gu and B. Vemuri. Matching 3D shapes using 2D conformal representations. In C. Barillot, D. R. Haynor, and P. Hellier, editors, *Medical Image Computing and Computer-Assisted Intervention, MICCAI*, pages 771–780, Sep. 2004.
- [15] W.M. Wells III, P. Viola, H. Atsumi, S. Nakajima, and R. Kikinis. Multi-modal volume registration by maximization of mutual information. *Medical Image Analysis*, 1(1):35–51, 1996.
- [16] J. West, J.M. Fitzpatrick, and M.Y. Wang et al. Comparison and evaluation of retrospective intermodality brain image registration techniques. *Journal of Computer Assisted Tomography*, 21(4):554–566, 1997.
- [17] C.R. Meyer, J.L. Boes, B. Kim, P.H. Bland, K.R. Zasadny, P.V. Kison, K. Koral, K.A. Frey, and R.L. Wahl. Demonstration of accuracy and clinical versatility of mutual information for automatic multimodality image fusion using affine and thin plate spline warped geometric deformation. *Medical Image Analysis*, 1(3):195–206, 1997.
- [18] D. Rueckert, L.I. Sonoda, C. Hayes, D.L.G. Hill, M.O. Leach, and D.J. Hawkes. Nonrigid registration using free-form deformations: application to breast mr images. *IEEE Transactions on Medical Imaging*, 18(8):712–721, 1999.
- [19] B. Kim, J.L. Boes, K.A. Frey, and C.R. Meyer. Mutual information for automated unwarping of rat brain autoradiographs. *NeuroImage*, 5:31–40, 1997.
- [20] G. Hermosillo. *Variational methods for multimodal image matching*. PhD thesis, Universit de Nice (INRIA-ROBOTVIS), Sophia Antipolis, France, 2002.
- [21] E. D’Agostino, F. Maes, D. Vandermeulen, and P. Suetens. A viscous fluid model for multimodal non-rigid image registration using mutual information. *Medical Image Analysis*, 7:565–575, 2003.
- [22] G.E. Christensen, R.D. Rabbitt, and M.I. Miller. Deformable templates using large deformation kinematics. *IEEE Transactions on Image Processing*, 5(10):1435–1447, 1996.
- [23] X. Gu, Y. Wang, and S.-T. Yau. Geometric compression using Riemann surface. *Communications in Information and Systems*, 3(3):171–182, 2005.
- [24] E. Parzen. On the estimation of probability density functions. *The annals of mathematical statistics*, 33:1065–1076, 1962.